HAL
open science

Source-free integration method for black hole perturbations and self-force computation: Radial fall

Sofiane Aoudia, Alessandro D.A.M. Spallicii

To cite this version:

Sofiane Aoudia, Alessandro D.A.M. Spallicii. Source-free integration method for black hole perturbations and self-force computation: Radial fall. Physical Review D, 2011, 83, pp.064029. 10.1103/PhysRevD.83.064029 . insu-01254554

HAL Id: insu-01254554

https://insu.hal.science/insu-01254554v1

Submitted on 12 Jan 2016

HAL is a multi-disciplinary open access archive for the deposit and dissemination of scientific research documents, whether they are published or not. The documents may come from teaching and research institutions in France or abroad, or from public or private research centers.

L'archive ouverte pluridisciplinaire **HAL**, est destinée au dépôt et à la diffusion de documents scientifiques de niveau recherche, publiés ou non, émanant des établissements d'enseignement et de recherche français ou étrangers, des laboratoires publics ou privés.

Distributed under a Creative Commons Attribution - NonCommercial - NoDerivatives 4.0 International License

PHYSICAL REVIEW D **83,** 064029 (2011)

Source-free integration method for black hole perturbations and self-force computation: Radial fall

Sofiane Aoudia*

Max Planck Institut für Gravitationphysik, A. Einstein, Golm 1 Am Mühlenberg 14476 Golm, Germany

Alessandro D. A. M. Spallicci†

Université d'Orléans, Observatoire des Sciences de l'Univers en région Centre OSUC, LPC2E-CNRS 3A Av. Recherche Scientifique 45071 Orléans, France

(Received 13 August 2010; published 21 March 2011)

Perturbations of Schwarzschild-Droste black holes in the Regge-Wheeler gauge benefit from the availability of a wave equation and from the gauge invariance of the wave function, but lack smoothness. Nevertheless, the even perturbations belong to the C^0 continuity class, if the wave function and its derivatives satisfy specific conditions on the discontinuities, known as jump conditions, at the particle position. These conditions suggest a new way for dealing with finite element integration in the time domain. The forward time value in the upper node of the (t, r^*) grid cell is obtained by the linear combination of the three preceding node values and of analytic expressions based on the jump conditions. The numerical integration does not deal directly with the source term, the associated singularities and the potential. This amounts to an indirect integration of the wave equation. The known wave forms at infinity are recovered and the wave function at the particle position is shown. In this series of papers, the radial trajectory is dealt with first, being this method of integration applicable to generic orbits of EMRI (Extreme Mass Ratio Inspiral).

DOI: 10.1103/PhysRevD.83.064029 PACS numbers: 04.25.Nx, 04.30.Db, 04.30.Nk, 04.70.Bw

I. INTRODUCTION

It is currently affirmed that the core of most galaxies host supermassive black holes, on which stars and compact objects in the neighborhood inspiral and plunge-in. The EMRI (Extreme Mass Ratio Inspiral) sources are characterized by a huge number of parameters that, when spanned over a large period, produce a huge number of templates for the LISA (Laser Interferometer Space Antenna) project [1]. Thus, matched filtering (the superposition of the expected and received signals) [2] is aided by stochastic methods [3]; in alternative, other more robust methods based on covariance or on time and frequency analysis are investigated [2,4–8]. Furthermore, if the signal from a capture is not individually detectable, it still may contribute to the statistical background [9,10]. Detection strategies are to be tested by the LISA simulators [11–13].

Challenges by EMRIs arise increasing interest amongst astrophysicists and those studying data analysis, but also for theorists. Relativists, especially, have been drawn to study EMRIs for the determination of the motion of the captured mass and because of the impact that back-action has on the gravitational wave forms (see [14] where a comprehensive introduction to these topics is given).

The captured compact object may be compared to a small mass m perturbing the background spacetime curvature of a large mass M and generating gravitational radiation. Perturbation methods from the seminal work of Regge and Wheeler, henceforth RW [15], were an obvious aid for studying the case we are dealing with. Approaches based on numerical relativity (NR) appear not be best suited, nor do the post-Newtonian (pN) expansions: the former for the two-scale problem (one small scale for the neighborhood of the particle, one large scale for the radiation at infinity); the latter for the small field and low velocity constraints. To EMRIs, nevertheless, Damour, Nagar, and coworkers [16–19], and Yunes [20] have applied the EOB (effective one body) method, though based on the pN approach. Furthermore, both pN and perturbation methods are found to be in agreement in their common domain of applicability by Blanchet *et al.* [21,22], as well as EOB and perturbation methods have shown their synergy thanks to Barack *et al.* [23]. Finally, it is to be mentioned that NR analysis is slowly progressing towards unequal mass ratios [24].

A. Perturbation methods

EMRIs have revived the interest for the perturbative relativistic two-body problem, which was investigated with a semirelativistic approach some 40 years ago by Ruffini and Wheeler [25,26], and then more fully by Zerilli [27–30]. These authors treated the source of the perturbations in the form of a radially falling particle. Zerilli's results opened the way for others to study to first order the orbital motion of the captured mass in a fully, although linearized, relativistic regime. Work done up until the end of the 1990s involved the captured star moving on

*aoudia@aei.mpg.de
†spallicci@cnrs-orleans.fr

 © 2011 American Physical Society

the geodesic of the background field and being unaffected by its own mass and the emitted radiation.

We shall refer to the first solution of the Einstein equation as the work of Droste [31–33] and Schwarzschild [34], collectively as SD, this double authorship having been justified by the historians, as recalled by Rothman [35]. Much research has been devoted to the study of SD black hole perturbations in the RW gauge, first in a vacuum [15], and then by Zerilli in the presence of a source [27–30]. An outflow of publications by Davis, Press, Price, Ruffini and Tiomno [36–41], but also by individual scholars like Chung [42], Dymnikova [43] appeared in the 1970s. It was followed by a slowdown in the 1980s and 1990s, with the exception of the forerunners of the Japanese school as Tashiro and Ezawa [44], Nakamura with Oohara and Koijma [45] or with Shibata [46]. The aim of all these authors was to analyze especially the amplitude and spectrum of the radiation emitted by the falling mass. Simulations were performed in frequency domain with the particle falling from infinity. The numerical accuracy was recently improved by Mitsou [47]. It was in 1997, that a fall from finite distance was analyzed by Lousto and Price [48]. The latter two authors were the first to use a finite difference scheme in time domain [49]. Following on this work, Martel and Poisson [50] were able to parametrize the initial conditions reflecting past motion of the particle and resulting into an initial amount of gravitational wave energy. All of this work was carried out in the RW gauge.

It is less than 15 years since we began to have methods for evaluating the back-action for point masses in strong fields thanks to two concurring situations. On one hand, the theorists progressed in understanding radiation reaction and obtained formal prescriptions for its determination. The solution was brought by the self-force equation, first by Mino, Sasaki and Tanaka [51], Quinn and Wald [52], and later by Detweiler and Whiting [53], all various approaches yielding the same formal expression. On the other hand, for the above-mentioned detection of captures, the requirements from LISA posed constraints on the tolerable amount of phase-shift on the wave forms, caused by radiation reaction. This impulse—project oriented—compelled the researchers to turn their efforts in finding an efficient and clear implementation of the prescription made by the theorists. The development was again pursued in perturbation theory. This time, though, the small mass m is correcting the geodesic equation of motion on a fixed background via a factor $\mathcal{O}(m)$.

Actually, the advances in the field by e.g. Warburton and Barack [54] and in radiation gauge by Keidl *et al.* [55] have recently tackled the self-force in Kerr geometry [56]. Such initial results in Kerr geometry do not mean that all major issues in nonrotating black holes have been solved. For instance, the self-consistent evolution of an orbit, along the lines suggested by Gralla and Wald [57], is not yet applied even to the simpler case of nonrotating black holes.

B. A different integration approach

The complexity in assessing the continuity of the perturbations (and the associated numerical computation of derivatives) at the position of the particle, has led Barack and Lousto [58], among other motivations such as the compatibility of the self-force to the (Lorenz-FitzGerald-de Donder) harmonic gauge [59–61], to convey their efforts to this gauge. This alternative enterprise is by no means priceless, the price being the unavailability of a wave equation like in the RW gauge and of the gauge invariance of the wave function, as determined by Moncrief [62]. In this context, the recent investigations of a gauge independent form of the self-force [63] may change sensibly the trade-off on the gauge choice.

The choice of a gauge should be suited to the type of problem under scrutiny and thus we do not adopt a position on which gauge should be preferred *a priori*. We find of some interest to revert a weakness of the RW gauge, namely, the lack of smoothness, into a building tool of a new integration method.

Indeed, we propose herein a finite element method of integration based on the jump conditions that the wave function and its derivatives have to satisfy for the SD black hole perturbations to be continuous at the position of the particle. We first deal with the radial trajectory and the associated even parity perturbations, while in a forthcoming paper [64] we shall present the circular and eccentric orbital cases, referring thus to both odd and even parity perturbations.

Herein, we present a first-order method and show that it suffices to acquire a well-behaved wave function at infinity and at the particle position. However, a higher order scheme has been derived and tested [65].

The main feature of the indirect (-I-) method consists in avoiding the explicit integration of the wave equation (the source term with the associated singularities and the potential) whenever the grid cells are crossed by the particle. Indeed, the information on the wave equation is implicitly given by the jump conditions. Conversely, for cells not crossed by the particle, we retain the classic approach for integrating wave equations [49,50], henceforth named LPMP.

For the computation of the back-action, the -I- method ensures a well-behaved wave function at the particle position, since the approach is governed by the theoretical values of the jump conditions.

C. Structure of the paper

The structure of the paper is as follows. Section II is a brief reminder of the formalism on perturbations for a SD black hole in the RW gauge. In Sec. III, we give an overview about the jump conditions on the wave function and

its derivatives. In Sec. IV, we introduce the scheme by detailing one of the four physical cases that a particle crossing the mesh cell during its infall may encounter, while for the other three similar cases we simply provide the final result. In Sec. V some wave forms at infinity are shown, discussed and compared to those obtained with the LPMP method. Furthermore, the theoretical and numerical jump conditions at the position of the particle are displayed and commented. In the conclusions, Sec. VI, the perspectives are addressed.

Geometric units ($G = c = 1$) are used, unless stated otherwise. The metric signature is $(-, +, +, +)$.

II. BLACK HOLE PERTURBATIONS

The Zerilli-Moncrief (ZM) equation rules even-parity waves in the presence of a source: a freely falling point particle that generates a perturbation for which the difference from the SD geometry is small. The energy-momentum tensor $T_{\mu\nu}$ is given by the integral of the world line of the particle, the integrand containing a four-dimensional invariant δ Dirac distribution for the representation of the point particle trajectory. The vanishing of the covariant divergence of $T_{\mu\nu}$ is guaranteed by the world line being a geodesic in the background SD geometry, represented by the metric tensor $g_{\mu\nu}$. Finally, the complete description of the emitted gravitational waves is given by the symmetric tensor $h_{\mu\nu} \ll g_{\mu\nu}$.

The formalism can be summarized as follows. Any symmetric covariant tensor can be expanded in spherical harmonics [29]. Because of the spherical symmetry of the SD field, the linearized field equations are cast in the form of a rotationally invariant operator on $h_{\mu\nu}$. This term is equated to the energy-momentum tensor, also expressed in spherical tensorial harmonics. That is

$$Q[h_{\mu\nu}] \propto T_{\mu\nu}[\delta(r_u)], \tag{1}$$

where the $\delta(r_u)$ Dirac distribution represents the point particle unperturbed trajectory r_u. The rotational invariance is used to separate out the angular variables in the field equations. For the spherical symmetry of the 2-dimensional manifold on which t, r are constants under rotation in the θ, ϕ sphere, the ten components of the perturbing symmetric tensor transform like three scalars, two vectors and one tensor:

$$h_{tt}, h_{tr}, h_{rr} \qquad (h_{t\theta}; h_{t\phi}), (h_{r\theta}; h_{r\phi}) \qquad \begin{pmatrix} h_{\theta\theta} & h_{\theta\phi} \\ h_{\phi\theta} & h_{\phi\phi} \end{pmatrix}.$$

In the Regge-Wheeler-Zerilli formalism, the source term for the odd perturbations vanishes for the radial trajectory and, given the rotational invariance through the azimuthal angle, only the index referring to the polar or latitude angle survives. The even perturbations, going as $(-1)^l$, are expressed by the following matrix

$$h_{\mu\nu} = \begin{pmatrix} \left(1 - \frac{2M}{r}\right) H_0^l Y^l & H_1^l Y^l & h_0^l Y^l_{,\theta} & h_0^l Y^l_{,\phi} \\ \text{sym} & \left(1 - \frac{2M}{r}\right)^{-1} H_2^l Y^l & h_1^l Y^l_{,\theta} & h_1^l Y^l_{,\phi} \\ \text{sym} & \text{sym} & r^2[K^l Y^l + G^l Y^l_{,\theta\theta}] & r^2 G^l (Y^l_{,\theta\phi} - \cot\theta Y^l_{,\phi}) \\ \text{sym} & \text{sym} & \text{sym} & r^2 \sin^2\theta \left[K^l + G^l \left(\frac{Y^l_{,\phi\phi}}{\sin^2\theta} + \cot\theta Y^l_{,\theta} \right) \right] \end{pmatrix}, \tag{2}$$

where H_0^l, H_1^l, H_2^l, h_0^l, h_1^l, K^l, G^l are functions of (t, r) and the spherical harmonics Y^l obviously of (θ, ϕ). Two formalisms describe the evolution of the perturbations in terms of a single wave function and a single wave equation. One, due to Moncrief [62], gauge invariant and developed about a 3-geometry of a $t =$ constant hypersurface, refers solely to the H_2^l, K^l, G^l, h_1^l, perturbations. The other, due to Zerilli [26–29], uses the RW gauge $G^l = h_0^l = h_1^l = 0$. In the RW gauge, the Moncrief wave function is given by

$$\Psi_l(t, r) = \frac{r}{\lambda + 1}\left[K^l + \frac{r - 2M}{\lambda r + 3M}\left(H_2^l - r\frac{\partial K^l}{\partial r} \right) \right], \tag{3}$$

where the Zerilli [28] normalization is used for Ψ_l. The dimension of the wave function is such that the energy is proportional to $\int_0^\infty \dot{\Psi}^2 dt$. Finally, the wave equation is given by

$$\frac{\partial^2 \Psi^l(t, r)}{\partial r^{*2}} - \frac{\partial^2 \Psi^l(t, r)}{\partial t^2} - V^l(r)\Psi^l(t, r) = S^l(t, r), \tag{4}$$

where $r^* = r + 2M \ln(r/2M - 1)$ is the tortoise coordinate. The potential $V^l(r)$ is expressed by

$$V^l(r) = \left(1 - \frac{2M}{r}\right) \times \frac{2\lambda^2(\lambda + 1)r^3 + 6\lambda^2 M r^2 + 18\lambda M^2 r + 18M^3}{r^3(\lambda r + 3M)^2}, \tag{5}$$

being $\lambda = 1/2(l - 1)(l + 2)$. The source $S^l(t, r)$ includes the derivative of the Dirac distribution, which appears in the process of building a single wave equation out of the seven even linearized wave equations

$$S^l = \frac{2(r-2M)\kappa}{r^2(\lambda+1)(\lambda r+3M)}\left\{\frac{r(r-2M)}{2U^0}\delta'[r-r_u(t)] - \left[\frac{r(\lambda+1)-3M}{2U^0} - \frac{3MU^0(r-2M)^2}{r(\lambda r+3M)}\right]\delta[r-r_u(t)]\right\}, \tag{6}$$

$U^0 = \sqrt{1-2M/r_{u0}}/(1-2M/r_u)$ being the time component of the 4-velocity and $\kappa = 4m\sqrt{(2l+1)\pi}$. The trajectory in the unperturbed SD metric $r_u(t)$ assumes different forms according to the initial conditions. For the radial infall of a particle starting from rest at finite distance r_{u0}, $r_u(t)$ is the inverse function of

$$\frac{t(r_u)}{2M} = \sqrt{1-\frac{2M}{r_{u0}}}\sqrt{1-\frac{r_u}{r_{u0}}}\left(\frac{r_{u0}}{2M}\right)\left(\frac{r_u}{2M}\right)^{1/2} + 2\,\mathrm{arctanh}\left(\frac{\sqrt{\frac{2M}{r_u}-\frac{2M}{r_{u0}}}}{\sqrt{1-\frac{2M}{r_{u0}}}}\right) + \sqrt{1-\frac{2M}{r_{u0}}}\left(1+\frac{4M}{r_{u0}}\right) \times \left(\frac{r_{u0}}{2M}\right)^{3/2}\arctan\left(\sqrt{\frac{r_{u0}}{r}-1}\right) \tag{7}$$

where $E = \sqrt{1-2M/r_{u0}}$.

For an infalling mass from infinity at zero velocity, the energy radiated to infinity for all modes [37] is given by (in physical units)

$$\sum_l E^l_{\mathrm{rad}} = 0.0104\frac{m^2c^2}{M}, \tag{8}$$

while most of the energy is emitted below the frequency

$$f_m = 0.08\frac{c^3}{GM}. \tag{9}$$

Up to 94% of the energy is radiated between $8M$ and $2M$ and 90% of it in the quadrupole mode. Obviously the above expressions would sensibly vary in case of an initial relativistic velocity.

For the SD black hole perturbations, there have been successive corrections of the basic equations, the last being pointed out by Sago, Nakano and Sasaki [66]. Sago *et al.* have corrected the ZM equations (a minus sign missing in all right-hand side terms) but introduced a wrong definition of the scalar product leading to errors in the coefficients of the energy-momentum tensor [67]. The expressions herein correspond to those in [68], where some of the errors of previously published literature on radial fall are indicated.

III. THE JUMP CONDITIONS

It has been indicated by two different heuristic arguments [69,70] that even metric perturbations, for radial fall in the RW gauge, should belong to the C^0 continuity class at the position of the particle. One argument [69] is based on the integration in r of the Hamiltonian constraint, which is the tt component of the Einstein equations (Eq. (C7a) in [30]); the other [70] on the structure of selected even perturbation equations. Following the latter, Lousto and Nakano evince the continuity of the even perturbations and afterwards impose such continuity to derive the jump conditions on the wave function and its derivatives for $l = 2$, notably starting from the ZM equation.

In this section, we instead provide an analysis *vis à vis* the jump conditions that the wave function and its derivatives have to satisfy for guaranteeing the continuity of the perturbations at the position of the particle. This approach [71] is based on the solutions of the ZM equation, not on the equation itself. The jump conditions found herein are applicable to all modes. Incidentally, the jump conditions were previously mentioned by Sopuerta and Laguna [72], Haas [73], and Field *et al.* [74] in a different context. In the forthcoming paper [64], the jump conditions for generic orbits are based on the analysis of the odd and even wave equations and are determined despite the lack of continuity of the perturbations.

In the radial case, only three independent perturbations survive, namely K^l, $H^l_0 = H^l_2$, H^l_1. The inverse relations for those perturbations, as functions of the wave function and its derivatives, are given by (we drop henceforth the l index)

$$K = \frac{6M^2+3M\lambda r+\lambda(\lambda+1)r^2}{r^2(\lambda r+3M)}\Psi + \left(1-\frac{2M}{r}\right)\Psi_{,r} - \frac{\kappa U^0(r-2M)^2}{(\lambda+1)(\lambda r+3M)r}\delta, \tag{10}$$

$$H_2 = -\frac{9M^3+9\lambda M^2 r+3\lambda^2 Mr^2+\lambda^2(\lambda+1)r^3}{r^2(\lambda r+3M)^2}\Psi + \frac{3M^2-\lambda Mr+\lambda r^2}{r(\lambda r+3M)}\Psi_{,r} + (r-2M)\Psi_{,rr} + \frac{\kappa U^0(r-2M)(\lambda^2r^2+2\lambda Mr-3Mr+3M^2)}{r(\lambda+1)(\lambda r+3M)^2}\delta - \frac{\kappa U^0(r-2M)^2}{(\lambda+1)(\lambda r+3M)}\delta', \tag{11}$$

$$H_1 = \frac{\lambda r^2-3M\lambda r-3M^2}{(r-2M)(\lambda r+3M)}\Psi_{,t} + r\Psi_{,tr} - \frac{\kappa U^0\dot{z}_u(\lambda r+M)}{(\lambda+1)(\lambda r+3M)}\delta + \frac{\kappa U^0\dot{z}_u r(r-2M)}{(\lambda+1)(\lambda r+3M)}\delta', \tag{12}$$

where $\delta = \delta[r-r_u(t)]$ and $\delta' = \delta'[r-r_u(t)]$.

From the visual inspection of the ZM wave equation (4), it is evinced that the wave function Ψ is of C^{-1} continuity class, since the second derivative of the wave function is proportional to the first derivative of the Dirac distribution (incidentally, the concept of C^{-1} continuity class element, like a Heaviside step distribution, may be pragmatically introduced as an element of a class of functions which after integration transforms into an element belonging to the C^0 class of functions). Thus, the wave function and its derivatives can be written as

$$\Psi = \Psi^+(t,r)\Theta_1 + \Psi^-(t,r)\Theta_2, \tag{13}$$

$$\Psi_{,r} = \Psi^+_{,r}\Theta_1 + \Psi^-_{,r}\Theta_2 + (\Psi^+ - \Psi^-)\delta, \tag{14}$$

$$\Psi_{,rr} = \Psi^+_{,rr}\Theta_1 + \Psi^-_{,rr}\Theta_2 + (\Psi^+_{,r} - \Psi^-_{,r})\delta + (\Psi^+ - \Psi^-)_{r_u}\delta', \tag{15}$$

$$\Psi_{,t} = \Psi^+_{,t}\Theta_1 + \Psi^-_{,t}\Theta_2 - (\Psi^+ - \Psi^-)\dot{r}_u\delta, \tag{16}$$

$$\Psi_{,tr} = \Psi^+_{,tr}\Theta_1 + \Psi^-_{,tr}\Theta_2 + (\Psi^+_{,t} - \Psi^-_{,t})\delta - (\Psi^+ - \Psi^-)_{r_u}\dot{r}_u\delta', \tag{17}$$

where $\Theta_1 = \Theta[r - r_u(t)]$, and $\Theta_2 = \Theta[r_u(t) - r]$ are two Heaviside step distributions. For Eqs. (15) and (17), a property of the Dirac delta distribution at the position of the particle, namely $f(r)\delta'[r - r_u(t)] = f|_{r_u(t)}\delta'[r - r_u(t)] - f'|_{r_u(t)}\delta[r - r_u(t)]$, has been used.

The wave function Ψ and its derivatives are to be replaced in Eqs. (10)–(12). At the position of the particle, it is wished that the combination of all discontinuities renders the perturbations of C^0 class. Thus, the coefficients of Θ_1 must be equal to the coefficients of Θ_2, while the coefficients of δ and δ' must vanish separately. To this end, the perturbations are expressed in an implicit form

$$K = f_1(r)\Psi + f_2(r)\Psi_{,r} + f_3(r)\delta, \tag{18}$$

$$H_2 = f_4(r)\Psi + f_5(r)\Psi_{,r} + f_6(r)\Psi_{,rr} + f_7(r)\delta + f_8(r)\delta', \tag{19}$$

$$H_1 = f_9(r)\Psi_{,t} + f_{10}(r)\Psi_{,tr} + f_{11}(r)\delta + f_{12}(r)\delta', \tag{20}$$

where the definitions of the f functions may be easily drawn by visual inspection of Eqs. (10)–(12). The jump conditions are obtained via Eq. (18)

$$(\Psi^+ - \Psi^-)_{r_u} = -\frac{f_3}{f_2}, \tag{21}$$

$$(\Psi^+_{,r} - \Psi^-_{,r})_{r_u} = \frac{f_1 f_3}{f_2^2}, \tag{22}$$

via Eq. (19)

$$(\Psi^+ - \Psi^-)_{r_u} = -\frac{f_8}{f_6}, \tag{23}$$

$$(\Psi^+_{,r} - \Psi^-_{,r})_{r_u} = \frac{1}{f_6}\left(\frac{f_5 f_8}{f_6} - f_7 + f_{8,r} - \frac{f_{6,r} f_8}{f_6}\right), \tag{24}$$

and finally via Eq. (20)

$$(\Psi^+ - \Psi^-)_{r_u} = \frac{f_{12}}{\dot{r}_u f_{10}}. \tag{25}$$

The jump conditions set by Eqs. (21), (23), and (25), are equivalent, as those set by Eqs. (22) and (24). The equivalence shows the consistency of the conditions and the compliance to the continuity requirement. The first t, second r, second mixed t, r derivative jump conditions (coming from H_2 and H_1) are given by

$$(\Psi^+_{,rr} - \Psi^-_{,rr})_{r_u} = -\frac{f_4(\Psi^+ - \Psi^-) + f_5(\Psi^+_{,r} - \Psi^-_{,r})}{f_6}, \tag{26}$$

$$(\Psi^+_{,t} - \Psi^-_{,t})_{r_u} = \frac{d(\Psi^+ - \Psi^-)}{dt} - (\Psi^+_{,r} - \Psi^-_{,r})\dot{r}_u = \frac{(f_9 - f_{10,r})\dot{r}_u(\Psi^+ - \Psi^-) - f_{11} + f_{12,r}}{f_{10}}, \tag{27}$$

$$(\Psi^+_{,tr} - \Psi^-_{,tr})_{r_u} = -\frac{f_9(\Psi^+_{,t} - \Psi^-_{,t})}{f_{10}}. \tag{28}$$

In explicit form, the jump conditions become

$$(\Psi^+ - \Psi^-)_{r_u} = \frac{\kappa E r_u}{(\lambda + 1)(3M + \lambda r_u)}, \tag{29}$$

$$(\Psi^+_{,r} - \Psi^-_{,r})_{r_u} = \frac{\kappa E[6M^2 + 3M\lambda r_u + \lambda(\lambda + 1)r_u^2]}{(\lambda + 1)(2M - r_u)(3M + \lambda r_u)^2}, \tag{30}$$

$$(\Psi^+_{,rr} - \Psi^-_{,rr})_{r_u} = -\frac{\kappa E[3M^3(5\lambda - 3) + 6M^2\lambda(\lambda - 3)r_u + 3M\lambda^2(\lambda - 1)r_u^2 - 2\lambda^2(\lambda + 1)r_u^3]}{(\lambda + 1)(2M - r_u)^2(3M + \lambda r_u)^3}, \tag{31}$$

$$(\Psi^+_{,t} - \Psi^-_{,t})_{r_u} = -\frac{\kappa E r_u \dot{r}_u}{(2M - r_u)(3M + \lambda r_u)}, \tag{32}$$

$$(\Psi^+_{,tr} - \Psi^-_{,tr})_{r_u} = \frac{\kappa E(3M^2 + 3M\lambda r_u - \lambda r_u^2)\dot{r}_u}{(2M - r_u)^2(3M + \lambda r_u)^2}. \tag{33}$$

Having established the jump conditions for any value of l at first order, we now turn to the presentation of the integration scheme. It is remarked that first derivatives of the jump conditions suffice to a scheme at first order.

IV. THE NUMERICAL METHOD

Our integration domain is discretized using a two-dimensional uniform mesh based on the coordinates t, r^* as depicted in Fig. 1, where $-450 < r^*/2M < 1000$ and $0 < t < t_{\rm end}$, with $t_{\rm end}$ greater than the falling time. Each cell has an area of $2h^2$ where $\sqrt{2}h$ is the dimension of an edge of the cell. The evolution scheme starts with the initial data approach by Martel and Poisson [50].

The numerical scheme

The jump conditions determined in the previous section are functions of the t, r variables, but for convenience in the following computations, they are transformed into functions of t, r^*. The integration method considers cells belonging to two groups: for cells which are never crossed by the particle, the integrating approach is drawn by the LPMP method, whereas for cells which are crossed, we propose our strategy.

There are four subcases representing the different particle trajectories inside the cell, see Figs. 2–5. We define α, β, γ, δ the four vertices of the diamond centered on σ and initially consider the world line crossing the cell as displayed in Fig. 2. The trajectory crosses the line β-δ at the point a and the line α-γ at the point b. We also define the shift ϵ_a and the lapse ϵ_b as $\epsilon_a = \min\{r^*_a - r^*_\beta, r^*_\delta - r^*_a\}$, $\epsilon_b = \min\{t_\alpha - t_b, t_b - t_\gamma\}$, respectively. The jump

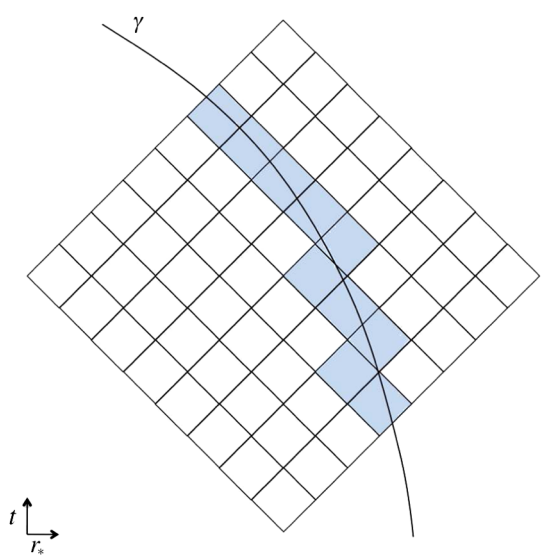

FIG. 1 (color online). Numerical domain: a staggered 1 + 1-dimensional mesh in t,r^* coordinates. The geodesic trajectory of the particle is represented by the continued line γ. The shadowed cells are those crossed by the particle.

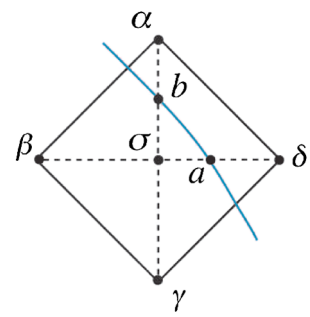

FIG. 2 (color online). Cell crossed by the particle. The particle crosses the segment $[\sigma\delta]$ at the point a and the segment $[\sigma\alpha]$ at the point b.

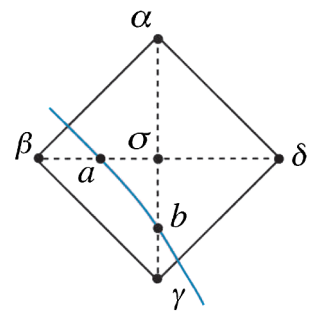

FIG. 3 (color online). Cell crossed by the particle. The particle crosses the segment $[\sigma\gamma]$ at the point b and the segment $[\sigma\beta]$ at the point a.

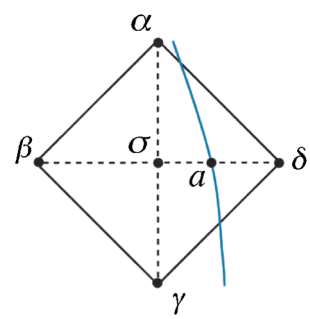

FIG. 4 (color online). Cell crossed by the particle. The particle crosses the segment $[\sigma\delta]$ at the point a.

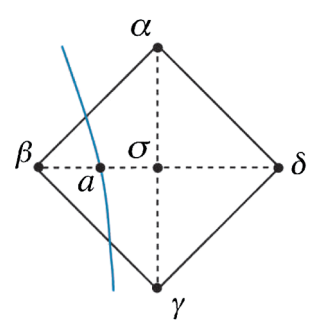

FIG. 5 (color online). Cell crossed by the particle. The particle crosses the segment $[\sigma\beta]$ at the point a.

conditions at the a, b coordinates express six analytical equations

$$(\Psi^+ - \Psi^-)_a = [\Psi]_a, \tag{34}$$

$$(\Psi^+ - \Psi^-)_b = [\Psi]_b, \tag{35}$$

$$(\Psi^+_{,r^*} - \Psi^-_{,r^*})_a = [\Psi_{,r^*}]_a, \tag{36}$$

$$(\Psi^+_{,r^*} - \Psi^-_{,r^*})_b = [\Psi_{,r^*}]_b, \tag{37}$$

$$(\Psi^+_{,t} - \Psi^-_{,t})_a = [\Psi_{,t}]_a, \tag{38}$$

$$(\Psi^+_{,t} - \Psi^-_{,t})_b = [\Psi_{,t}]_b. \tag{39}$$

We maintain the superscript notation for which the wave function values between the world line and infinity are noted by the plus sign, and conversely by the minus sign for the values between the world line and the horizon (incidentally, such notation would also be applicable to the LPMP method).

Using a first-order expansion, we get a set of six numerical equations. For case 1, see Fig. 2, they are

$$\Psi^+_\alpha = \Psi^+(t_b + \epsilon_b, r^*_b) = \Psi^+_b + \epsilon_b \Psi^+_{,t}|_b, \tag{40}$$

$$\Psi^-_\sigma = \Psi^-(t_b - (h - \epsilon_b), r^*_b) = \Psi^-_b - (h - \epsilon_b)\Psi^-_{,t}|_b, \tag{41}$$

$$\begin{aligned}\Psi^-_\gamma &= \Psi^-(t_b - 2h + \epsilon_b, r^*_b) = \Psi^-(t_\sigma - h, r^*_b)\\ &= \Psi^-_\sigma - h\Psi^-_{,t}|_\sigma,\end{aligned} \tag{42}$$

$$\Psi^+_\delta = \Psi^+(t_a, r^*_a + \epsilon_a) = \Psi^+_a + \epsilon_a \Psi^+_{,r^*}|_a, \tag{43}$$

$$\Psi^-_\sigma = \Psi^-(t_a, r^*_a - (h - \epsilon_a)) = \Psi^-_a - (h - \epsilon_a)\Psi^-_{,r^*}|_a, \tag{44}$$

$$\begin{aligned}\Psi^-_\beta &= \Psi^-(t_a, r^*_a - 2h + \epsilon_a) = \Psi^-(t_\sigma, r^*_\sigma - h)\\ &= \Psi^-_\sigma - h\Psi^-_{,r^*}|_\sigma.\end{aligned} \tag{45}$$

Our aim is the determination of the value of Ψ^+_α, knowing those of Ψ^-_β, Ψ^-_γ, Ψ^+_δ, ϵ_a, ϵ_b, $[\Psi]_{a,b}$, $[\Psi_{,r}]_{a,b}$ and $[\Psi_{,t}]_{a,b}$ To this end, we subtract Eq. (41) from Eq. (40), Eq. (44) from Eq. (43) and obtain, respectively

$$\Psi^+_\alpha = \Psi^-_\sigma + [\Psi]_b + \epsilon_b[\Psi_{,t}]_b + h\Psi^-_{,t}|_b, \tag{46}$$

$$\Psi^+_\delta = \Psi^-_\sigma + [\Psi]_a + \epsilon_a[\Psi_{,r^*}]_a + h\Psi^-_{,r^*}|_a. \tag{47}$$

Summing Eq. (42), (46), (45), and (47), and combining the results, we finally get

$$\begin{aligned}\Psi^+_\alpha = \Psi^-_\beta - \Psi^-_\gamma + \Psi^+_\delta - [\Psi]_a + [\Psi]_b - \epsilon_a[\Psi_{,r^*}]_a\\ + \epsilon_b[\Psi_{,t}]_b.\end{aligned} \tag{48}$$

We thus have obtained, without direct integration of the singular source, the value of the upper node. Furthermore, the latter depends solely on analytic expressions, and obviously on the other values at the cell corners. Similar relations are found for the other three cases. For case 2 (Fig. 3), we obtain

$$\begin{aligned}\Psi^+_\alpha = \Psi^-_\beta - \Psi^-_\gamma + \Psi^+_\delta + [\Psi]_a - [\Psi]_b - \epsilon_a[\Psi_{,r^*}]_a\\ + \epsilon_b[\Psi_{,t}]_b;\end{aligned} \tag{49}$$

for case 3 (Fig. 4)

$$\Psi^-_\alpha = \Psi^-_\beta - \Psi^-_\gamma + \Psi^+_\delta - [\Psi]_a - \epsilon_a[\Psi_{,r^*}]_a; \tag{50}$$

for case 4 (Fig. 5)

$$\Psi^+_\alpha = \Psi^-_\beta - \Psi^+_\gamma + \Psi^+_\delta + [\Psi]_a - \epsilon_a[\Psi_{,r^*}]_a. \tag{51}$$

In a concise form, the four cases might be represented by a single expression (where Ψ_α stands for Ψ^+_α or Ψ^-_α, and Ψ_γ stands for Ψ^+_γ or Ψ^-_γ)

$$\begin{aligned}\Psi_\alpha = \Psi^-_\beta - \Psi_\gamma + \Psi^+_\delta \mp \{[\Psi]_a - B[\Psi]_b\} - \epsilon_a[\Psi_{,r^*}]_a\\ + B\epsilon_b[\Psi_{,t}]_b,\end{aligned} \tag{52}$$

where the upper sign holds when $r^*_a > r^*_\sigma$ and the lower when $r^*_a < r^*_\sigma$, $B = 0$ if the particle does not cross the α-γ line, and $B = 1$ otherwise.

V. RADIATED WAVE FORMS AT INFINITY AND THE WAVE FUNCTION AT THE PARTICLE

We confirm the existing wave forms previously published by Lousto and Price [49], and Martel and Poisson [50]. In this section, the results from a code based on the LPMP method (full second order) are compared to those obtained by the -I- method (first order for the filled cells, as presented herein, and LPMP-like for empty cells). In spite of the partially different order of the two codes, the difference between the wave forms computed by the two methods is marginal. Incidentally, this occurs in absence of a recognized standard to which refer different numerical approaches.

Figures 6 and 7 show the $l = 2$ wave forms for the LPMP and -I- methods, for a particle falling radially, with zero initial velocity, from $r_{u0}/2M = 5$ and $r_{u0}/2M = 20$, respectively, in units $u = t - r^*$, $(2M/m)\Psi$. The initial data are given by the minimal ($\alpha = 1$) initial data condition $H_2 = \alpha K$ for both cases (the parameter α, introduced in [50], measures the amount of radiation present on the initial hypersurface and for $\alpha = 1$, the initial metric is conformally flat).

Figures 8 and 9 show the logarithmic (absolute) difference for the $l = 2$ wave forms between the LPMP and -I- methods, for a particle falling radially, with zero initial velocity, from $r_{u0}/2M = 5$ and $r_{u0}/2M = 20$, respectively. It is evinced that the normalized wave function amplitudes differ of an amount between 10^{-3} and $10^{-8.5}$, in normalized units.

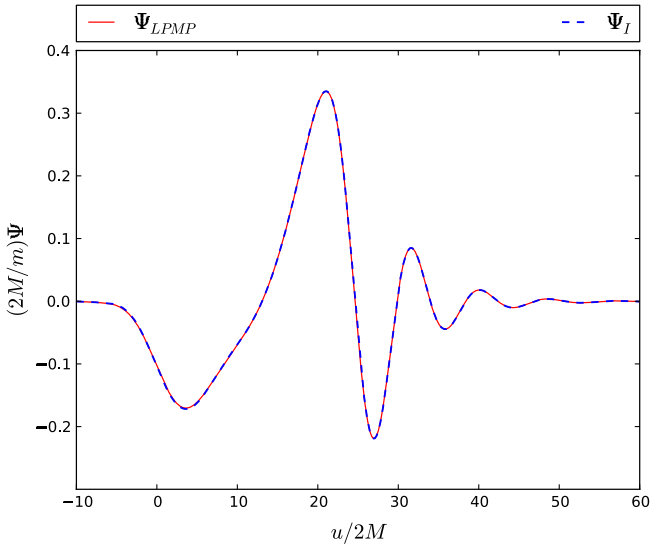

FIG. 6 (color online). Radiated $l = 2$ wave form for a particle falling radially from $r_{u0}/2M = 5$ with zero initial velocity, in units $u = t - r^*$, $(2M/m)\Psi$. The dashed and solid line represent the -I- and LPMP methods, respectively.

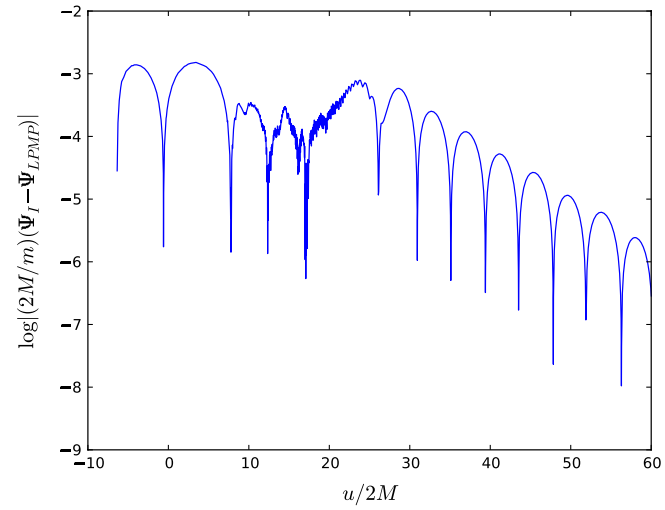

FIG. 8 (color online). Logarithmic (absolute) difference plot for a particle falling radially from $r_{u0}/2M = 5$ with zero initial velocity, in units $u = t - r^*$, $(2M/m)\Psi$, between the -I- and LPMP methods ($l = 2$).

We show also the behavior of the wave function at the position of the particle, Figs. 10 and 11. The theoretical jump condition, Eq. (29), and the numerical result well overlap at the particle position, as it may be inferred from the logarithmic (absolute) difference plots, Figs. 12 and 13. The discrepancy in normalized units is between 10^{-3} and $10^{-6.5}$.

Discussion

The features of the -I- method can be summarized as follows:

(i) For the grid cells crossed by the particle, direct and explicit integration of the wave equation, the source term with the associated singularities and the potential, is avoided. This determines also a faster code.

(ii) Reliability is improved, since analytic expressions totally replace the numerical expressions representing the source. The terminology "source-free" is due to this feature.

(iii) A higher order scheme can be written, starting from a higher order Taylor expansion for Eqs. (40)–(45), and associated to this method [65].

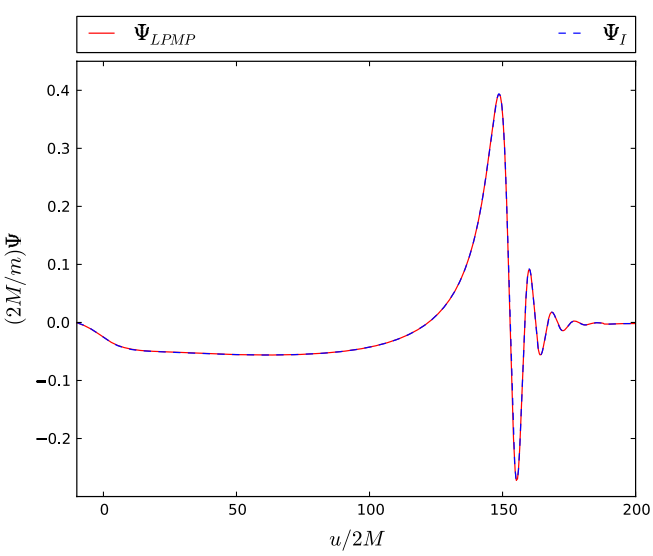

FIG. 7 (color online). Radiated $l = 2$ wave form for a particle falling radially from $r_{u0}/2M = 20$ with zero initial velocity, in units $u = t - r^*$, $(2M/m)\Psi$. The dashed and solid line represent the -I- and LPMP methods, respectively.

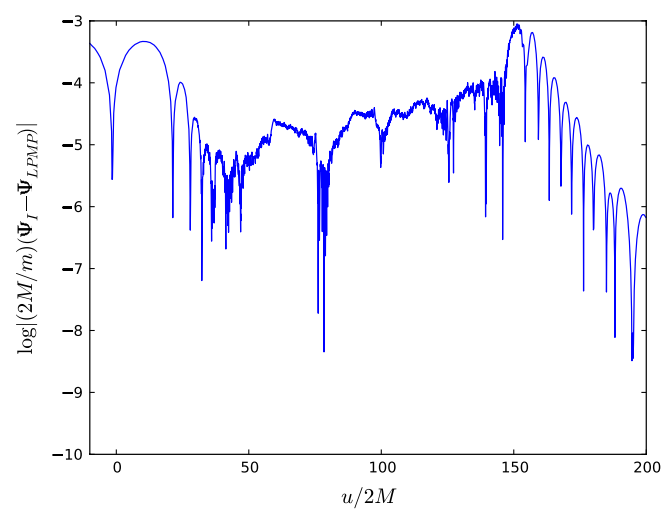

FIG. 9 (color online). Logarithmic (absolute) difference plot for a particle falling radially from $r_{u0}/2M = 20$ with zero initial velocity, in units $u = t - r^*$, $(2M/m)\Psi$, between the -I- and LPMP methods ($l = 2$).

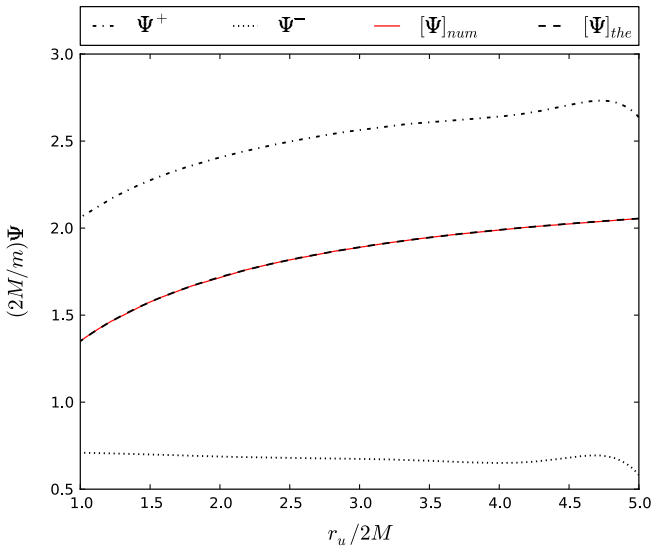

FIG. 10 (color online). Wave function (Ψ^+, dashed-dotted line, and Ψ^-, dotted line) at the particle position for a particle falling radially from $r_{u0}/2M = 5$ with zero initial velocity ($l = 2$), in units $u = t - r^*$, $(2M/m)\Psi$. The numerical jump condition $[\Psi]_{\rm num}$, solid line, and the theoretical jump condition $[\Psi]_{\rm the}$, dashed line Eq. (29), are shown.

(iv) The applicability of the method stretches out to generic orbits. It is our concern to apply the -I-method to circular and eccentric orbits, even if these orbits are not accompanied by perturbations of C^0 class. The rationale poses on the following consideration. Instead of using the continuity of the perturbations to get the jump conditions, we assume that the even and odd wave equations are satisfied by Ψ, respectively R, being C^{-1}. Using this approach, we have obtained encouraging results for an eccentric orbit [64].

(v) The disadvantage of this method is represented by the four possible trajectories that a particle may follow inside a given cell, instead of the three possible paths of the LPMP method. A different labeling of the intersections between the particle world line and the cell, though, reduces the number of cases to three [65].

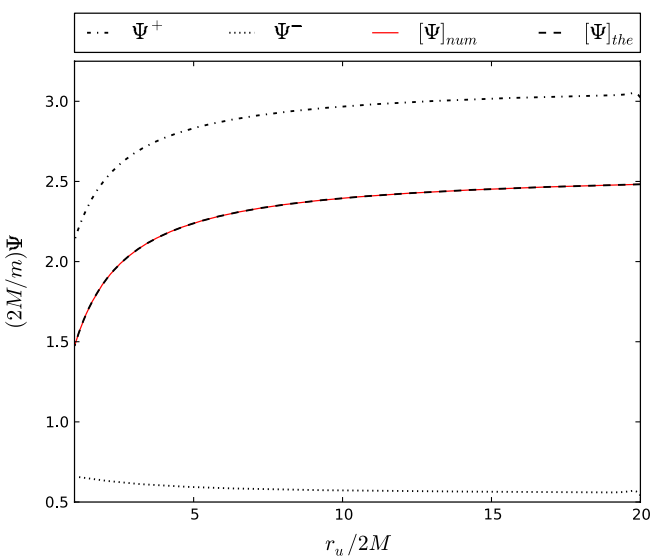

FIG. 11 (color online). Wave function (Ψ^+, dashed-dotted line, and Ψ^-, dotted line) at the particle position for a particle falling radially from $r_{u0}/2M = 20$ with zero initial velocity ($l = 2$), in units $u = t - r^*$, $(2M/m)\Psi$. The numerical jump condition $[\Psi]_{\rm num}$, solid line, and the theoretical jump condition $[\Psi]_{\rm the}$, dashed line Eq. (29), are shown.

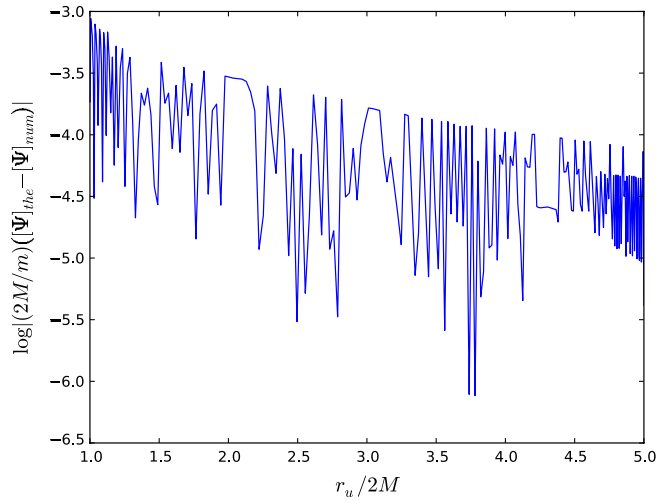

FIG. 12 (color online). Logarithmic (absolute) difference plot for a particle falling radially from $r_{u0}/2M = 5$ with zero initial velocity, in units $u = t - r^*$, $(2M/m)\Psi$, at the particle position, between theoretical and numerical jump conditions ($l = 2$).

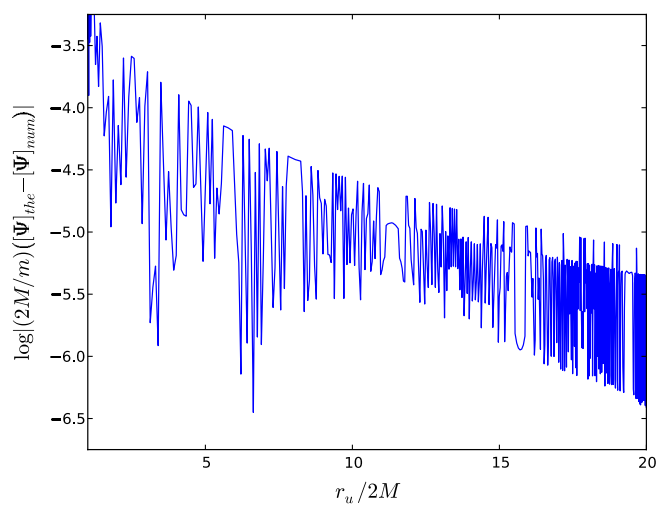

FIG. 13 (color online). Logarithmic (absolute) difference plot for a particle falling radially from $r_{u0}/2M = 20$ with zero initial velocity, in units $u = t - r^*$, $(2M/m)\Psi$, at the particle position, between theoretical and numerical jump conditions ($l = 2$).

VI. CONCLUSIONS AND OUTLOOK

We have presented a novel integration method in the time domain for the Zerili-Moncrief wave equation at first order, for cells crossed by the particle world line. The forward time value in the upper node of the (t, r^*) grid cell is obtained by the linear combination of the three preceding node values and of the analytic jump conditions. Therefore, the numerical integration does not deal any longer with the source term, the associated singularities and the potential. The direct integration of the wave equation is circumvented.

The wave forms at infinity confirm published results, and the wave function at the particle position shows a well-behaved pattern. Our final aim is the evaluation and the application of the back-action at the position of the particle, in a self-consistent manner.

The indirect or source-free method has been developed to fourth order [65] and applied to generic orbits [64].

Beyond the scenario of EMRIs, other lines of investigation may emerge. One concerns the formal relation between the algorithms of the indirect and LPMP approaches [49,50]. Another considers applicability of the indirect method to all wave equations with a singular source term, and which the wave function of is constrained by a set of properties.

ACKNOWLEDGMENTS

Discussions with Stéphane Cordier (MAPMO-Orléans), Marc-Thierry Jaekel (LPT ENS—Paris), José Martin-Garcia (now at Wolfram Research) and Patxi Ritter (doctorate student—Orléans) have clarified the jump conditions. Support from the latter in coding and producing the figures is acknowledged. John Alexander Tully, astronomer at the Observatoire de la Cote d'Azur in Nice, is thanked for reading the manuscript. Helpful comments from the referee were appreciated and implemented. The authors wish to acknowledge the FNAK (Fondation Nationale Alfred Kastler), the C. J. C. (Confédération des Jeunes Chercheurs) and all organizations which stand against discrimination of foreign researchers.

[1] LISA websites. http://lisa.jpl.nasa.gov, http://www.esa.int/science/lisa.
[2] B. S. Sathyaprakash and B. F. Schutz, Classical Quantum Gravity **20**, S209 (2003).
[3] E. K. Porter, arXiv:0910.0373v1.
[4] J. R. Gair and G. Jones, Classical Quantum Gravity **24**, 1145 (2007).
[5] J. R. Gair, I. Mandel, and L. Wen, J. Phys. Conf. Ser. **122**, 012037 (2008).
[6] J. R. Gair, I. Mandel, and L. Wen, Classical Quantum Gravity **25**, 184031 (2008).
[7] N. J. Cornish, arXiv:0804.3323v3.
[8] S. Babak, J. R. Gair, and E. K. Porter, Classical Quantum Gravity **26**, 135004 (2009).
[9] L. Barack and C. Cutler, Phys. Rev. D **70**, 122002 (2004).
[10] E. Racine and C. Cutler, Phys. Rev. D **76**, 124033 (2007).
[11] N. J. Cornish and L. J. Rubbo, Phys. Rev. D **67**, 022001 (2003); **67**029905(E) (2003).
[12] M. Vallisneri, Phys. Rev. D **71**, 022001 (2005).
[13] A. Petiteau, G. Auger, H. Halloin, O. Jeannin, E. Plagnol, S. Pireaux, T. Regimbau, and J.-Y. Vinet, Phys. Rev. D **77**, 023002 (2008).
[14] L. Blanchet, A. Spallicci, and B. Whiting, *Mass and Motion in General Relativity* (Springer, Berlin, 2011).
[15] T. Regge and J. A. Wheeler, Phys. Rev. **108**, 1063 (1957).
[16] A. Nagar, T. Damour, and A. Tartaglia, Classical Quantum Gravity **24**, S109 (2007).
[17] T. Damour and A. Nagar, Phys. Rev. D **76**, 064028 (2007).
[18] S. Bernuzzi and A. Nagar, Phys. Rev. D **81**, 084056 (2010).
[19] T. Damour, Phys. Rev. D **81**, 024017 (2010).
[20] N. Yunes, A. Buonanno, S. A. Hughes, M. C. Miller, and Y. Pan, Phys. Rev. Lett. **104**, 091102 (2010).
[21] L. Blanchet, S. Detweiler, A. Le Tiec, and B. F. Whiting, Phys. Rev. D **81**, 064004 (2010).
[22] L. Blanchet, S. Detweiler, A. Le Tiec, and B. F. Whiting, Phys. Rev. D **81**, 084033 (2010).
[23] L. Barack, T. Damour, and N. Sago, Phys. Rev. D **82**, 084036 (2010).
[24] U. Sperhake, *Theory Meets Data Analysis at Comparable and Extreme Mass Ratios* (Perimeter Institute, Waterloo, Canada, 2010).
[25] R. Ruffini and J. A. Wheeler, in *Significance of Space Research for Fundamental Physics, ESRO Colloquium, Interlaken 1969, ESRO-52*, edited by A. F. Moore and V. Hardy (European Space Research Organisation, Paris, 1971), p. 45.
[26] R. Ruffini and J. A. Wheeler, in *The Astrophysical Aspects of the Weak Interactions, Cortona 1970, ANL Quaderno n. 157*, edited by G. Bernardini, E. Amaldi, and L. Radicati di Brozolo (Accademia Nazionale dei Lincei, Roma, 1971), p. 165.
[27] F. J. Zerilli, Ph.D. thesis, Princeton University, 1969.
[28] F. J. Zerilli, Phys. Rev. Lett. **24**, 737 (1970).
[29] F. J. Zerilli, J. Math. Phys. (N.Y.) **11**, 2203 (1970).
[30] F. J. Zerilli, Phys. Rev. D **2**, 2141 (1970); in *Black Holes, Les Houches 1972,* edited by C. DeWitt and B. DeWitt (Gordon and Breach Science Publ., New York, 1973).
[31] J. Droste, Kon. Ak. Wetensch. Amsterdam **23**, 968 (1915); [Proc. Acad. Sci. Amsterdam **17**, 998 (1915)].

[32] J. Droste, Doctorate thesis, Rijksuniversiteit van Leiden, 1916.
[33] J. Droste, Kon. Ak. Wetensch. Amsterdam **25**, 163 (1916); [Proc. Acad. Sci. Amsterdam **19**, 197 (1917)].
[34] K. Schwarzschild, Sitzungsber. Preuss. Akad. Wiss., Phys. Math. Kl., 189 (1916); S. Antoci and A. Loinger, arXiv: physics/9905030v1.
[35] T. Rothman, Gen. Relativ. Gravit. **34**, 1541 (2002).
[36] M. Davis and R. Ruffini, Lett. Nuovo Cimento **2**, 1165 (1971).
[37] M. Davis, R. Ruffini, W. H. Press, and R. H. Price, Phys. Rev. Lett. **27**, 1466 (1971).
[38] M. Davis, R. Ruffini, and J. Tiomno, Phys. Rev. D **5**, 2932 (1972).
[39] R. Ruffini, in *Black Holes, Les Houches 1972*, edited by C. DeWitt and B. DeWitt (Gordon and Breach Science, New York, 1973), p. 451.
[40] R. Ruffini, Phys. Rev. D **7**, 972 (1973).
[41] R. Ruffini, in *Proceedings of Int. School of Phys. E. Fermi Course LXV, Varenna 1975*, edited by R. Giacconi and R. Ruffini (North-Holland, Amsterdam and Soc. It. Fisica, Bologna, 1978), p. 287.
[42] K. P. Chung, Nuovo Cimento B **14**, 293 (1973).
[43] I. G. Dymnikova, Yad. Fiz. **31**, 679 (1980) [Sov. J. Nucl. Phys. **31**, 353 (1980)].
[44] Y. Tashiro and H. Ezawa, Prog. Theor. Phys. **66**, 1612 (1981).
[45] T. Nakamura, K. Oohara, and Y. Koijma, Prog. Theor. Phys. Suppl. **90**, 1 (1987).
[46] M. Shibata and T. Nakamura, Prog. Theor. Phys. **87**, 1139 (1992).
[47] E. Mitsou, arXiv:1012.2028v2.
[48] C. O. Lousto and R. H. Price, Phys. Rev. D **55**, 2124 (1997).
[49] C. O. Lousto and R. H. Price, Phys. Rev. D **56**, 6439 (1997).
[50] K. Martel and E. Poisson, Phys. Rev. D **66**, 084001 (2002).
[51] Y. Mino, M. Sasaki, and T. Tanaka, Phys. Rev. D **55**, 3457 (1997).
[52] T. C. Quinn and R. M. Wald, Phys. Rev. D **56**, 3381 (1997).
[53] S. Detweiler and B. F. Whiting, Phys. Rev. D **67**, 024025 (2003).
[54] N. Warburton and L. Barack, Phys. Rev. D **81**, 084039 (2010).
[55] T. S. Keidl, A. G. Shah, J. L. Friedman, D.-H. Kim, and L. R. Price, Phys. Rev. D **82**, 124012 (2010).
[56] R. P. Kerr, Phys. Rev. Lett. **11**, 237 (1963).
[57] S. E. Gralla and R. M. Wald, Classical Quantum Gravity **25**, 205009 (2008).
[58] L. Barack and C. O. Lousto, Phys. Rev. D **72**, 104026 (2005).
[59] L. Lorenz, Philos. Mag. Ser. 4 **34**, 287 (1867).
[60] B. J. Hunt, *The Maxwellians* (Cornell University Press, New York, 1991).
[61] T. de Donder, *La gravifique Einsteinienne* (Gauthier-Villars, Paris, 1921).
[62] V. Moncrief, Ann. Phys. (N.Y.) **88**, 323 (1974).
[63] S. Gralla, *Theory Meets Data Analysis at Comparable and Extreme Mass Ratios* (Perimeter Institute, Waterloo, Canada, 2010).
[64] S. Aoudia and A. Spallicci (unpublished).
[65] P. Ritter, A. Spallicci, S. Aoudia, and S. Cordier, Classical Quantum Gravity (to be published).
[66] N. Sago, H. Nakano, and M. Sasaki, Phys. Rev. D **67**, 104017 (2003).
[67] H. Nakano (private communication).
[68] A. Spallicci, in *Mass and Motion in General Relativity*, edited by L. Blanchet, A. Spallicci, and B. Whiting (Springer, Berlin, 2011).
[69] C. O. Lousto, Phys. Rev. Lett. **84**, 5251 (2000).
[70] C. O. Lousto and H. Nakano, Classical Quantum Gravity **26**, 015007 (2009).
[71] S. Aoudia and A. Spallicci, in *12th Marcel Grossmann Meeting, Paris 2009*, edited by T. Damour, R. T. Jantzen, and R. Ruffini (World Scientific, Singapore, 2011).
[72] C. F. Sopuerta and P. Laguna, Phys. Rev. D **73**, 044028 (2006).
[73] R. Haas, Phys. Rev. D **75**, 124011 (2007).
[74] S. E. Field, J. S. Hesthaven, and S. R. Lau, Classical Quantum Gravity **26**, 165010 (2009).